

## The Neoproterozoic-Early Cambrian felsic magmatism in Calabria (Italy): inferences as to the origin and geodynamic setting

ANNAMARIA FORNELLI, FRANCESCA MICHELETTI\* and GIUSEPPE PICCARRETA

Dipartimento Geomineralogico, Università degli Studi di Bari, Via E. Orabona, 4, 70125, Bari, Italy

**ABSTRACT.** — Some of the Alpine Units of the nappe pile of Calabria (southern Italy) include blocks of Variscan continental crust. Among these, the Castagna, Sila and Aspromonte Units containing felsic augen gneisses are here considered. These augen gneisses are abundant in the Castagna and Aspromonte Units, whereas are scarce in the lower crust segment of the Sila Unit. Spot U-Pb zircon-dating revealed Latest Precambrian-Early Cambrian emplacement of the magmatic protoliths of the augen gneisses from the three units with Neoproterozoic, Palaeoproterozoic and Archean inheritances. Geochemistry and Sr, Nd isotope signatures indicate the protoliths formed in orogenic setting through mixing of crust-mantle melts. The high-K calc-alkaline to shoshonitic nature of protoliths points to a transition between compressive and extensional tectonic setting or even to a collapsed intracontinental orogen formed by amalgamated Cadomian terranes and Gondwana craton. The coeval emplacement of similar melts in the three different units suggests they were portions of the same Pan-African-Cadomian block in Precambrian times. Sr and Nd isotope signatures evidence that these magmas cannot be derived

from the partial melting of the now exposed restitic metapelites of the lower crust segment of the Sila Unit. More likely the basement containing the augen gneisses was eradicated from the source of the crustal melts during the Variscan orogeny and records recycled terranes derived from West African Craton.

**RIASSUNTO.** — Alcune Unità Alpine costituenti l'edificio a falde in Calabria (Italia meridionale) includono importanti porzioni di crosta continentale Varisca. Fra queste, le Unità di Castagna, della Sila e dell'Aspromonte sono caratterizzate dalla presenza di ortoderivati acidi costituiti essenzialmente da gneiss occhiadini. Questi sono presenti diffusamente nelle Unità di Castagna e dell'Aspromonte, mentre formano corpi esigui all'interno della porzione di crosta profonda dell'Unità della Sila. Datazioni puntuali U-Pb su zirconi, selezionati da campioni provenienti dalle tre unità, indicano che gli gneiss occhiadini sono ascrivibili a voluminose intrusioni al limite Neoproterozoico superiore-Cambriano inferiore, conservando eredità Neoproterozoiche, Paleoproterozoiche ed Archeane. I caratteri geochimici ed isotopici (sistematiche Rb-Sr e Sm-Nd) evidenziano un ambiente geodinamico di tipo orogenico e la natura ibrida dei protoliti. Il carattere calc-alcinalo ricco in K di tali prodotti indicherebbe un regime tettonico transizionale

\* Corresponding author, E-mail:  
[f.micheletti@geomun.uniba.it](mailto:f.micheletti@geomun.uniba.it)

tra compressivo ed estensionale, o legato al collasso di un orogene intracontinentale derivante dall'amalgamazione di terreni Cadomiani con il Gondwana. La presenza di magmatiti acide coeve e geochimicamente simili entro differenti porzioni di crosta continentale varisca suggerisce che queste porzioni crostali appartenevano allo stesso blocco Pan-Africano-Cadomiano. Gli gneiss occhiadini hanno connotati isotopici che rendono improbabile la derivazione dei protoliti dalla fusione parziale, al limite Precambriano-Cambriano, delle metapeliti restitiche di crosta profonda oggi affioranti nell'Unità della Sila. Probabilmente i terreni contenenti gli gneiss occhiadini sono stati sradicati durante l'orogenesi Varisca dalle rocce sorgenti dei fusi crostali.

KEY WORDS: *Augen gneisses, geochemistry, U-Pb zircon data, Precambrian blocks, Calabria.*

#### INTRODUCTION

In Calabria, the Alpine s.l. nappe pile contains remnants of pre-Variscan crustal blocks, including felsic and mafic orthoderivates. The pre-Variscan pertinence is so far documented in the Castagna, Sila and Aspromonte Units by: conventional U-Pb zircon ages and Rb-Sr isochron (Schenk, 1980; Schenk, 1989; Schenk and Todt, 1989; Senesi, 1999); spot U-Pb zircon ages (Micheletti *et al.* 2007; Fornelli *et al.*, 2007 and unpubl. data) and fossiliferous records (Acquafredda *et al.*, 1994 and references therein). Neoproterozoic-Cambrian ages have been determined in the felsic augen gneisses occurring within the three units and Devonian-Carboniferous fossiliferous records occur in the very low-grade Palaeozoic volcano-sedimentary sequences overlying and welded to the segment of lower crust of the Sila Unit by Late-Carboniferous granitoids. Large volumes of felsic augen gneisses occur within the Castagna and Aspromonte Units, whereas only few decametre-sized bodies are present in the Sila Unit. The composition of the augen gneisses, which derived from felsic protoliths, gives new data useful: 1) to infer the origin of the felsic magmas, 2) to determine the geodynamic context in which this important magmatism occurred, and 3) to understand the possible location of the future Variscan Calabria terrains

along the northern margin of Gondwana. The conclusions have benefitted of both published and new original data.

#### GEOLOGICAL SETTING

The Calabria-Peloritani belt is an "exotic terrane" mainly consisting of tectonic units stacked during the Alpine s.l. orogenesis (e.g. Bonardi *et al.*, 2001; Festa *et al.*, 2004 and references therein). Among the tectonic units, Variscan continental rocks dominate in the Castagna, Aspromonte and Sila Units, that will be here considered (Figs. 1 and 2). They include pre-Variscan remnants constituted by metaigneous and metasedimentary rocks (Schenk, 1989; Schenk and Todt, 1989; Senesi, 1999; Micheletti *et al.*, 2007; Fornelli *et al.*, 2007 and unpubl. data). The Castagna Unit crops out from the northern Serre to the Catena Costiera (Fig. 1) and consists of micaschists, paragneisses, amphibolites and large volumes of felsic orthogneisses, among which augen gneisses are the most abundant (Colonna and Piccarreta, 1976; Paglionico and Piccarreta, 1976), intruded by Late-Carboniferous granitoids (e.g. Borsi and Dubois, 1968; Messina *et al.*, 1994). The Aspromonte Unit crops out in southern Calabria and in Peloritani mounts of Sicily (Fig. 1). It consists of amphibolite- to granulite-facies metaigneous and metasedimentary rocks intruded by Late-Carboniferous granitoids (Bonardi *et al.*, 1984 and references therein; Graessner and Schenk, 1999): the metaigneous rocks are felsic and mafic orthogneisses having pre-Cambrian igneous protoliths (Grande and Micheletti, 2006, and unpubl. data; Micheletti *et al.*, 2007 and references therein). The Sila Unit is exposed in Catena Costiera, Sila and Serre Massifs (Fig. 1). In the Serre, it includes (from bottom to top): i) 7-8 km thick metamorphites of the Variscan lower crust (Schenk, 1984); ii) a 10-12 km thick (Caggianelli and Prosser, 2002) Late-Carboniferous sheet-like granitoid bodies (Schenk, 1980) and iii) upper crust rocks in which very low-grade Palaeozoic volcano-sedimentary sequences preserve fossiliferous records (Acquafredda *et al.*, 1994). The Variscan

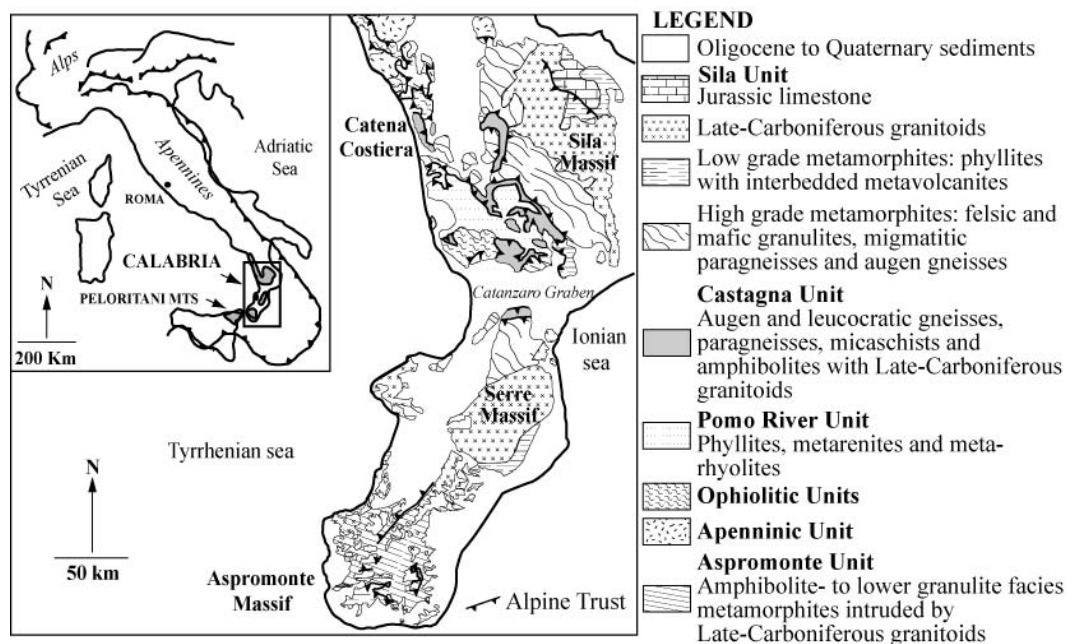


Fig. 1 – Geological sketch map of Calabria.

lower crust consists of metagabbros, mafic and felsic granulites at the base and prevalent migmatitic metapelites in the upper part. Small lenticular bodies of augen gneisses are present in the upper migmatitic metapelites. Secondary Ion Mass Spectrometry (SIMS) U-Pb analyses on magmatic zircons from the augen gneisses have given concordant and subconcordant ages ranging from 541 Ma to 556 Ma in the Castagna Unit, from 550 Ma to 586 Ma and from 522 Ma to 531 Ma in the Sila Unit and from 537 Ma to 572 Ma in the Aspromonte Unit (Micheletti *et al.*, 2007). Some zircon crystals show recrystallized luminescent cores younger than the rims having concordant ages in the range 446–494 Ma. Similar recrystallized domains with same ages occur also in the metasediments of the lower crustal rocks from the Sila Unit (Fornelli *et al.*, 2007, and unpubl. data). These values are consistent with the Rb-Sr isochron age of 450 Ma determined for the same metasediments by Schenk (1989). Neoproterozoic, Palaeoproterozoic and Archean inheritances (crystal cores giving concordant ages or upper intercept of U-Pb discordia

lines) are present in the augen gneisses from the three units (Micheletti *et al.*, 2007); the inherited ages determined in the metasediments of the lower crustal segment of the Sila Unit are younger than  $1688 \pm 36$  Ma (Fornelli *et al.*, 2007, and unpubl. data). The lower intercepts of U-Pb discordia lines obtained by spot analyses of magmatic zircons from the augen gneisses from the three Units range from  $526 \pm 10$  Ma to  $562 \pm 15$  Ma with the largest spread in the Aspromonte Unit; these ages similar to the concordant spot ages, have been interpreted as emplacement ages of the magmatic protoliths into a likely older basement (Micheletti *et al.*, 2007). All these rocks underwent intense Variscan reworking under lower-amphibolite (Castagna Unit) to granulite facies conditions (Sila Unit) as shown by zircon growth and/or recrystallization between 340 Ma and 260 Ma in the lower crustal metasediments and metagabbros from the Sila Unit (Fornelli *et al.*, 2007, and unpubl. data) and in the amphibole-bearing gneisses from the Aspromonte Unit (Grande and Micheletti, 2006, and unpubl. data).

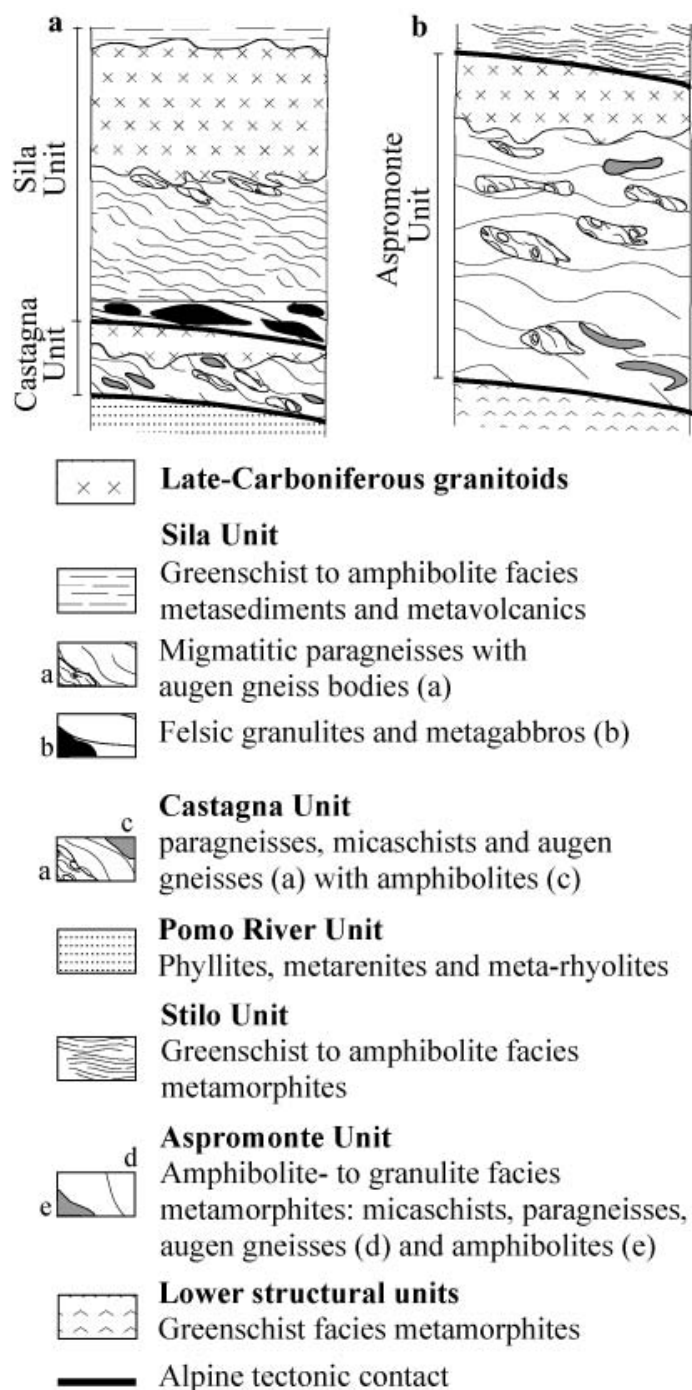


Fig. 2 – Sketch geologic sections through Sila and northern Serre massifs (a) and the Aspromonte massif (b).

## GEOCHEMICAL DATA

Samples unaffected by visible alteration have been selected on the base of the petrographic study. The representative samples (more than 6-7 kg) have been analysed. Thirty-nine samples were analysed for major (XRF at Bari University) and some trace elements (at CRPG-CNRS, Nancy, France); sixteen samples for rare earth elements (REE) and five for Sm-Nd and Rb-Sr isotope systematics (at CRPG-CNRS, Nancy, France); these data were taken from Micheletti *et al.* (2007). Sixteen other samples from Castagna and Sila Units were analysed only for major and trace elements (XRF at Bari University). The compositional means of augen gneisses from each unit are given in Table 1 and 2 and the analytical data points have been plotted in selected binary and ternary diagrams. From petrographic observations the studied samples result to have granodioritic and granitic compositions, consistently with the Zr/TiO<sub>2</sub> vs. Nb/Y diagram (Fig. 3A). However, in the A'KF diagram (Fig. 3B) many samples plot outside the granodiorite-granite field; in the CaO, Na<sub>2</sub>O, K<sub>2</sub>O vs. SiO<sub>2</sub> binary plots (Fig. 4) the Castagna and Aspromonte augen gneisses show a large spread of the oxides relative to a given silica content; and, on the average, CaO wt% < MgO wt% (Table 1). These features suggest a possible role of the chemical alteration. However, 1) the

(CaO+Na<sub>2</sub>O+K<sub>2</sub>O)/(Al<sub>2</sub>O<sub>3</sub>+TiO<sub>2</sub>+FeO+MgO) ratio, which ranges on average between 0.45 and 0.55, is quite similar to the range shown, on the average, by chemically comparable intrusive and extrusive rocks (Le Maitre *et al.*, 1989); 2) Al<sub>2</sub>O<sub>3</sub> and TiO<sub>2</sub>, which should show a positive correlation with the alteration degree, do not show covariance (Fig. 4) and the Al<sub>2</sub>O<sub>3</sub>/TiO<sub>2</sub> ratio varies from 14 to 23, from 20 to 37 and from 24 to 43, with higher values at higher silica contents, in Sila, Castagna and Aspromonte Units, respectively. These features exclude significant chemical alteration and general petrogenetic considerations are viable. In the analysed samples, the spread of K<sub>2</sub>O, Na<sub>2</sub>O and CaO appears to be positively correlated with the amount of the original feldspar phenocrysts, reflecting their inhomogeneous distribution in the protoliths. In particular, if we consider the K<sub>2</sub>O vs. SiO<sub>2</sub> plot (Fig. 4), it appears that, excluding the tails of the K<sub>2</sub>O-distribution, more than 65% of the samples of each unit straddles the high K-calcalkaline and shoshonitic fields as confirmed by the steep LREE patterns (see below).

The chondrite normalized REE patterns of the augen gneisses from all studied units are quite similar (Fig. 5A). They show fractionated LREE, strong negative Eu anomaly and flat HREE (Table 2, Fig. 5A). Element-abundances normalized to pyrolite (Fig. 5B)

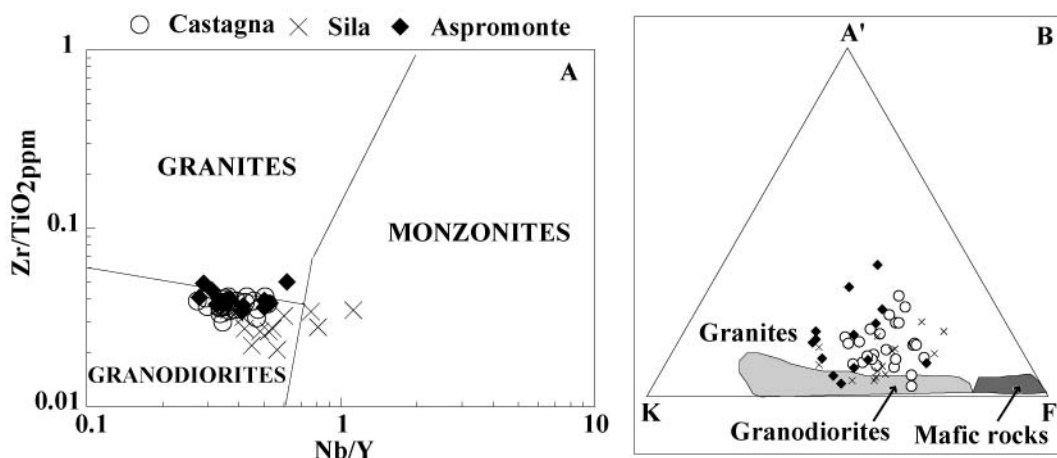


Fig. 3 – (A) Zr/TiO<sub>2</sub> vs. Nb/Y plot (Bozkurt *et al.*, 1995); (B) A'KF plot: A' = Al<sub>2</sub>O<sub>3</sub>-K<sub>2</sub>O-Na<sub>2</sub>O-CaO; K = K<sub>2</sub>O; F = (FeO+MgO-TiO<sub>2</sub>) as molar proportions.

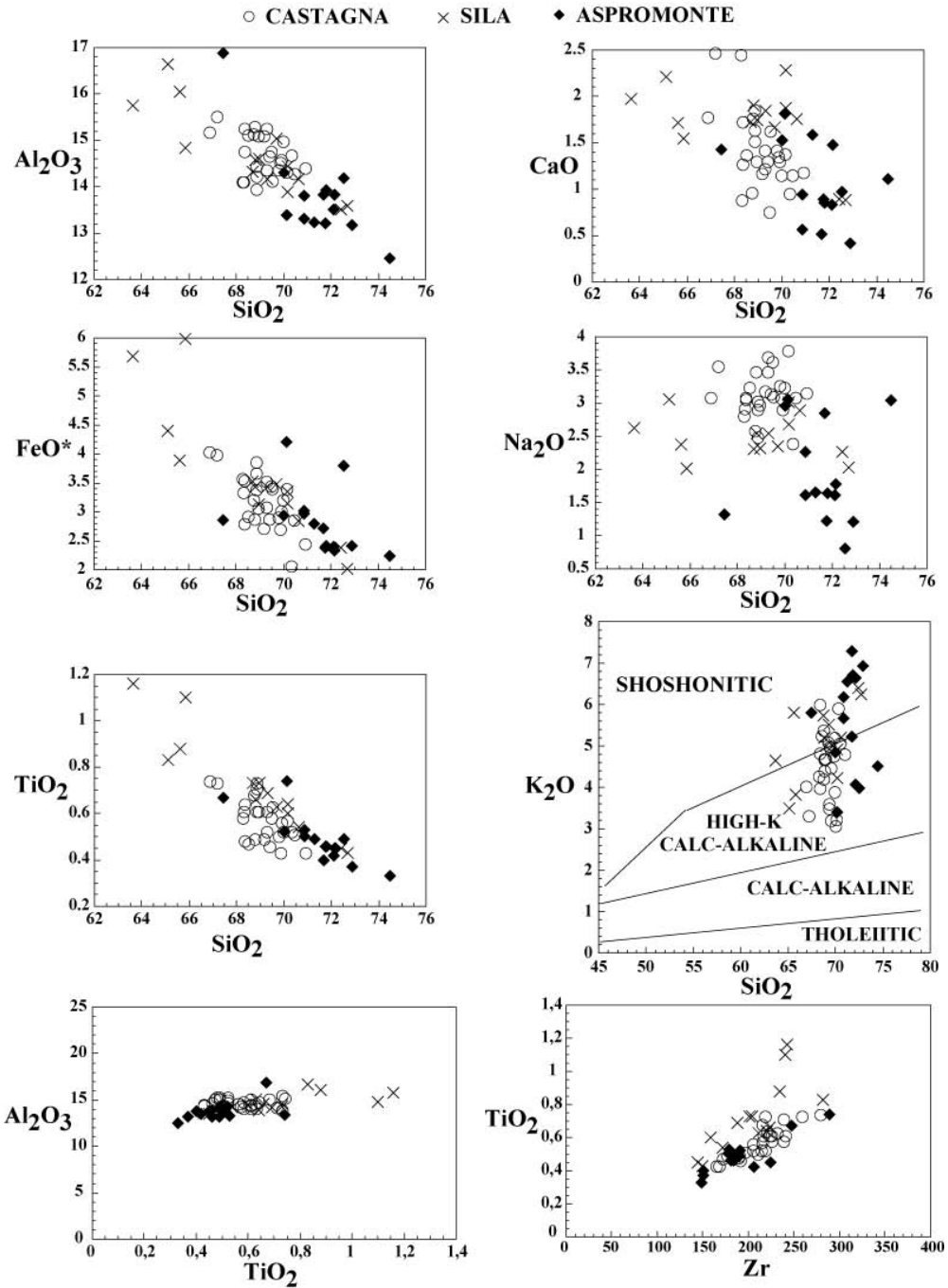


Fig. 4 – Some oxides vs.  $SiO_2$  plots,  $Al_2O_3$  vs.  $TiO_2$  and  $TiO_2$  vs.  $Zr$  plots (MACLEAN and BARRET, 1993) for the studied augen

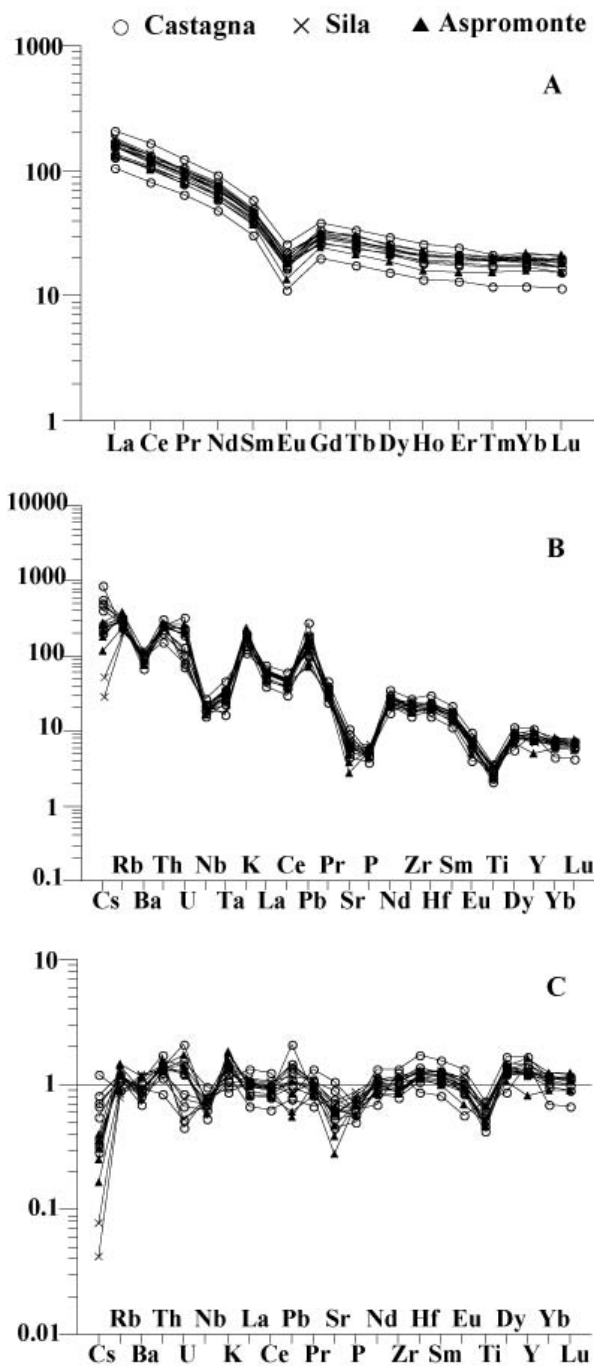


Fig. 5 – (A) Chondrite normalized REE patterns (McDonough and Sun, 1995); (B) Pyrolite normalized spiderdiagram (McDonough and Sun, 1995); (c) PAAS normalized spiderdiagram (Taylor and McLennan, 1985).

TABLE 1 – Means ( $X$ ) and ranges of major and trace elements of the augen gneisses from the Calabria ( $n$ =number of samples)

| wt%                            | Castagna Unit |              |        | Sila Unit |        |       | Aspromonte Unit |        |       |
|--------------------------------|---------------|--------------|--------|-----------|--------|-------|-----------------|--------|-------|
|                                | X (n=27)      | range        |        | X (n=14)  | range  |       | X (n=14)        | range  |       |
| SiO <sub>2</sub>               | 69.12         | 66.88-       | 70.92  | 68.71     | 63.65- | 72.71 | 71.43           | 67.46- | 74.50 |
| TiO <sub>2</sub>               | 0.57          | 0.43-        | 0.74   | 0.72      | 0.43-  | 1.16  | 0.49            | 0.33-  | 0.74  |
| Al <sub>2</sub> O <sub>3</sub> | 14.69         | 13.94-       | 15.51  | 14.68     | 13.50- | 16.65 | 13.79           | 12.46- | 16.88 |
| FeO                            | 3.18          | 2.07-        | 4.04   | 3.62      | 2.02-  | 5.99  | 2.82            | 2.23-  | 4.21  |
| MnO                            | 0.05          | 0.03-        | 0.08   | 0.05      | 0.01-  | 0.08  | 0.05            | 0.02-  | 0.09  |
| MgO                            | 1.53          | 0.91-        | 2.07   | 1.82      | 0.88-  | 3.47  | 1.20            | 0.56-  | 2.06  |
| CaO                            | 1.42          | 0.75-        | 2.47   | 1.72      | 0.88-  | 2.28  | 1.07            | 0.42-  | 1.82  |
| Na <sub>2</sub> O              | 3.12          | 2.39-        | 3.79   | 2.50      | 2.01-  | 3.05  | 1.93            | 0.80-  | 3.05  |
| K <sub>2</sub> O               | 4.46          | 3.06-        | 6.00   | 5.08      | 3.48-  | 6.41  | 5.56            | 3.39-  | 7.29  |
| P <sub>2</sub> O <sub>5</sub>  | 0.11          | 0.07-        | 0.16   | 0.10      | 0.03-  | 0.17  | 0.11            | 0.08-  | 0.12  |
| LOI                            | 1.41          | 0.73-        | 3.65   | 0.60      | 0.23-  | 1.46  | 1.24            | 0.59-  | 1.78  |
| ppm                            |               |              |        |           |        |       |                 |        |       |
| Ba                             | 645           | 453-         | 1099   | 739       | 519-   | 1358  | 560             | 194-   | 815   |
| Rb                             | 176           | 130-         | 262    | 131       | 98-    | 188   | 191             | 120-   | 246   |
| Sr                             | 136           | 87-          | 210    | 147       | 94-    | 258   | 94              | 39-    | 183   |
| Y                              | 38            | 30-          | 51     | 25        | 8-     | 39    | 33              | 19-    | 45    |
| Zr                             | 213           | 165-         | 279    | 205       | 144-   | 282   | 193             | 149-   | 289   |
| Nb                             | 14            | 10-          | 18     | 13        | 9-     | 16    | 13              | 10-    | 21    |
| V                              | 50            | 38- 68(n=17) |        | 58        | 30-    | 110   | 40              | 19-    | 68    |
| Cr                             | 62            | 38- 94(n=17) |        | 49        | 25-    | 141   | 36              | 16-    | 60    |
| Ni                             | 16            | 10-          | 22     | 15        | 9-     | 32    | 12              | 5-     | 25    |
| La                             | 31.14         | 22.00-       | 50.10  | 32.13     | 20.00- | 58.00 | 35.32           | 27.80- | 48.90 |
| Ce                             | 60.36         | 40.00-       | 101.00 | 56.56     | 31.90- | 93.00 | 65.00           | 44.80- | 81.10 |
| ppm                            |               |              |        |           |        |       |                 |        |       |
| Pr                             | X (n=9)       | range        |        | X (n=2)   | range  |       | X (n=5)         | range  |       |
| Pr                             | 8.60          | 5.99-        | 11.70  | 9.60      | 9.55-  | 9.64  | 8.48            | 7.34-  | 9.40  |
| Nd                             | 32.01         | 22.10-       | 43.00  | 35.40     | 35.30- | 35.50 | 31.10           | 26.90- | 34.50 |
| Sm                             | 6.50          | 4.55-        | 8.69   | 7.13      | 7.12-  | 7.13  | 6.42            | 5.48-  | 7.13  |
| Eu                             | 1.05          | 0.63-        | 1.44   | 1.20      | 1.16-  | 1.24  | 0.99            | 0.76-  | 1.06  |
| Gd                             | 5.83          | 3.99-        | 7.61   | 6.27      | 6.26-  | 6.27  | 5.73            | 4.80-  | 6.53  |
| Tb                             | 0.95          | 0.63-        | 1.20   | 1.00      | 1.00-  | 1.00  | 0.96            | 0.77-  | 1.10  |
| Dy                             | 5.75          | 3.77-        | 7.40   | 5.77      | 5.76-  | 5.78  | 5.64            | 4.58-  | 6.40  |
| Ho                             | 1.11          | 0.74-        | 1.43   | 1.14      | 1.13-  | 1.15  | 1.12            | 0.89-  | 1.24  |
| Er                             | 3.12          | 2.11-        | 3.89   | 3.21      | 3.18-  | 3.23  | 3.14            | 2.50-  | 3.45  |
| Tm                             | 0.46          | 0.30-        | 0.54   | 0.47      | 0.47-  | 0.48  | 0.48            | 0.38-  | 0.52  |
| Yb                             | 2.91          | 1.93-        | 3.31   | 3.19      | 3.15-  | 3.22  | 3.18            | 2.53-  | 3.53  |
| Lu                             | 0.43          | 0.29-        | 0.50   | 0.48      | 0.47-  | 0.49  | 0.47            | 0.38-  | 0.53  |
| Be                             | 3.40          | 1.71-        | 5.54   | 0.89      | 0.89-  | 0.89  | 2.14            | 0.87-  | 2.80  |
| Co                             | 7.34          | 5.51-        | 9.40   | 9.24      | 8.50-  | 9.99  | 6.92            | 6.00-  | 8.45  |
| Cs                             | 8.79          | 4.28-        | 18.30  | 0.90      | 0.63-  | 1.17  | 4.44            | 2.46-  | 5.94  |
| Ga                             | 19.02         | 11.00-       | 21.20  | 19.10     | 18.90- | 19.30 | 19.68           | 18.00- | 20.40 |
| Hf                             | 6.17          | 4.30-        | 8.69   | 6.10      | 5.99-  | 6.21  | 5.89            | 5.62-  | 6.40  |
| Pb                             | 24.00         | 15.00-       | 42.00  | 25.00     | 23.00- | 28.00 | 16.42           | 10.80- | 21.30 |
| Sn                             | 4.43          | 1.68-        | 7.72   | 0.59      | 0.49-  | 0.68  | 6.59            | 4.62-  | 9.03  |
| Ta                             | 1.10          | 0.60-        | 1.68   | 0.80      | 0.72-  | 0.88  | 1.14            | 1.01-  | 1.23  |
| Th                             | 19.00         | 12.00-       | 25.00  | 19.90     | 19.30- | 20.50 | 20.18           | 18.70- | 22.50 |
| U                              | 3.44          | 1.40-        | 6.49   | 1.99      | 1.64-  | 2.35  | 4.38            | 3.92-  | 5.30  |
| W                              | 10.63         | 3.78-        | 6.50   | 20.55     | 19.00- | 22.10 | 17.86           | 9.50-  | 45.40 |
| Zn                             | 58.00         | 19.00-       | 107.00 | 70.00     | 61.00- | 79.00 | 32.00           | 23.00- | 42.00 |



TABLE 2  
Some chemical parameters for the augen gneisses from Calabria

|          | Castagna Unit |             | Sila Unit |             | Aspromonte Unit |             |
|----------|---------------|-------------|-----------|-------------|-----------------|-------------|
|          | X             | range       | X         | range       | X               | range       |
|          | n=27          |             | n=14      |             | n=14            |             |
| A/CNK    | 1.18          | 1.03-1.39   | 1.16      | 1.04-1.45   | 1.26            | 1.04-1.92   |
| A/NK     | 1.48          | 1.32-1.73   | 1.54      | 1.27-1.99   | 1.55            | 1.26-2.53   |
| Mg-value | 45.99         | 39.34-56.84 | 46.12     | 39.22-55.81 | 42.35           | 29.22-56.28 |
| K/Rb     | 213           | 110-300     | 327       | 229-424     | 243             | 201-299     |
|          | n=9           |             | n=2       |             | n=5             |             |
| ΣHREE    | 20.56         | 13.76-25.74 | 21.52     | 21.42-21.62 | 20.73           | 16.83-23.02 |
| Eu/Eu*   | 0.52          | 0.45-0.58   | 0.55      | 0.53-0.57   | 0.5             | 0.45-0.57   |

show significant negative anomalies for Ba, Nb, Ta, Sr, P and Ti, and positive anomalies for Th, U, and K whereas Pb is variable. The PAAS (Post Archean Australian Shales, Taylor and McLennan, 1985) normalized elemental plot (Fig.5C) shows negative anomalies for Cs, Nb, Sr, P, Ti, and positive anomalies for Rb, K, whereas variable correlations for U and Pb; the other elements show abundances similar to PAAS. Similarities also exist as to the positive

and negative anomalies between the pyrolyte and the PAAS normalized patterns.

The  $^{87}\text{Sr}/^{86}\text{Sr}$  isotopic ratios and the  $\epsilon\text{Nd}$  values of the five analysed augen gneisses (Table 3), calculated at 540 Ma (the approximate emplacement age of the protoliths of the augen gneisses), are in the range 0.70856-0.71338 and between -3.2 and -4.6, respectively, and the  $\text{Nd}_{\text{DM}}$  model ages are quite homogeneous between 1.5 and 1.7 Ga (Table 3).

TABLE 3  
*Sm-Nd and Rb-Sr isotopic compositions of augen gneisses.  $\epsilon\text{Sr}$  and  $\epsilon\text{Nd}$  values are calculated at 540 Ma. CHUR and DM are from DE PAOLO and WASSERBURG (1976)*

| Sample                 | Rb  | Sr  | $^{87}\text{Rb}/^{86}\text{Sr}$ | $^{87}\text{Sr}/^{86}\text{Sr}$ | $(^{87}\text{Sr}/^{86}\text{Sr})_{540\text{Ma}}$ | $\epsilon\text{Sr}_{540\text{Ma}}$ | Nd   | Sm  | $^{147}\text{Sm}/^{144}\text{Nd}$ | $^{143}\text{Nd}/^{144}\text{Nd}$ | $\epsilon\text{Nd}_{540\text{Ma}}$ | $T_{\text{DM}}$ |
|------------------------|-----|-----|---------------------------------|---------------------------------|--|------------------------------------|------|-----|-----------------------------------|-----------------------------------|------------------------------------|-----------------|
| <i>Castagna Unit</i>   |     |     |                                 |                                 |  |                                    |      |     |                                   |                                   |                                    |                 |
| GO 6                   | 175 | 181 | 2.79                            | 0.73372                         | 0.71224  | 118.94                             | 35   | 6.9 | 0.11897                           | 0.5122                            | -3.18                              | 1.53            |
| GO 35                  | 190 | 156 | 3.51                            | 0.73557                         | 0.70856  | 66.49                              | 22.1 | 4.6 | 0.12454                           | 0.51216                           | -4.35                              | 1.69            |
| <i>Sila Unit</i>       |     |     |                                 |                                 |  |                                    |      |     |                                   |                                   |                                    |                 |
| GO 71                  | 136 | 154 | 2.55                            | 0.7301                          | 0.71047  | 93.76                              | 35.5 | 7.1 | 0.12132                           | 0.51215                           | -4.32                              | 1.65            |
| GO 100                 | 125 | 148 | 2.44                            | 0.73216                         | 0.71338  | 135.06                             | 35.3 | 7.1 | 0.12218                           | 0.51214                           | -4.58                              | 1.68            |
| <i>Aspromonte Unit</i> |     |     |                                 |                                 |  |                                    |      |     |                                   |                                   |                                    |                 |
| ADR 5                  | 237 | 132 | 5.18                            | 0.74968                         | 0.70981  | 84.32                              | 31.9 | 6.7 | 0.12705                           | 0.51218                           | -4.13                              | 1.7             |
| ADR 18                 | -   | -   | -                               | -                               | -  | -                                  | 26.9 | 5.5 | 0.12323                           | 0.51219                           | -3.67                              | 1.61            |

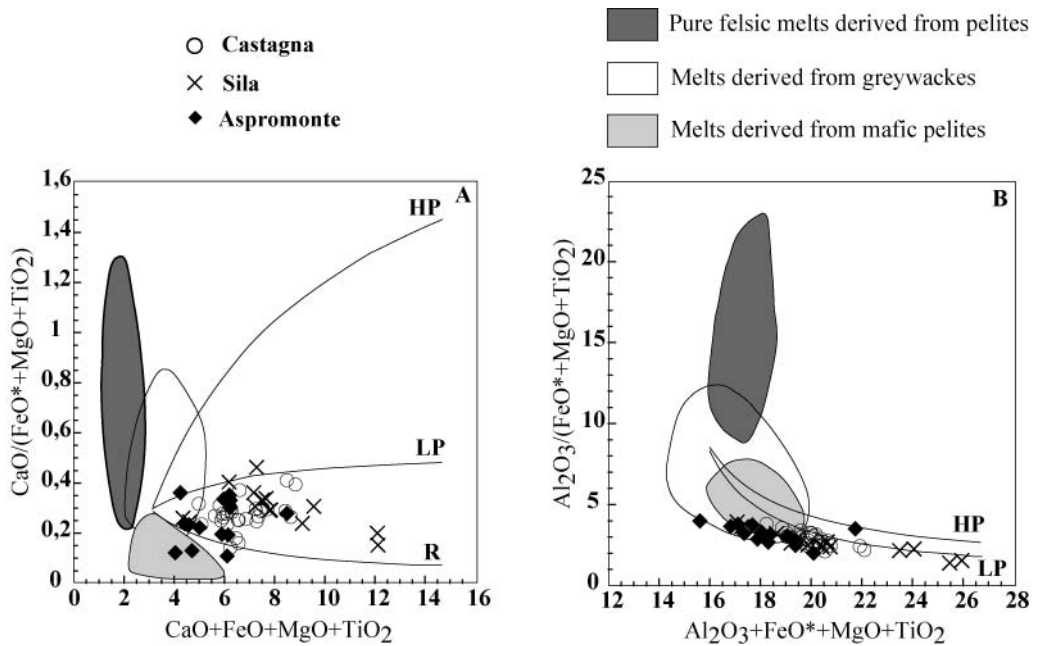


Fig. 6 – Composition of augen gneisses compared with melts produced by experimental dehydration-melting of various kinds of metasediments (Patino Douce, 1999). The high pressure (HP) and low pressure (LP) lines are reaction curves modeling the melt compositions produced by hybridization of high-Al olivine tholeiite and metapelite-derived melts; the R line shows the magma composition resulting from melt-restite mixing in a pelitic system.

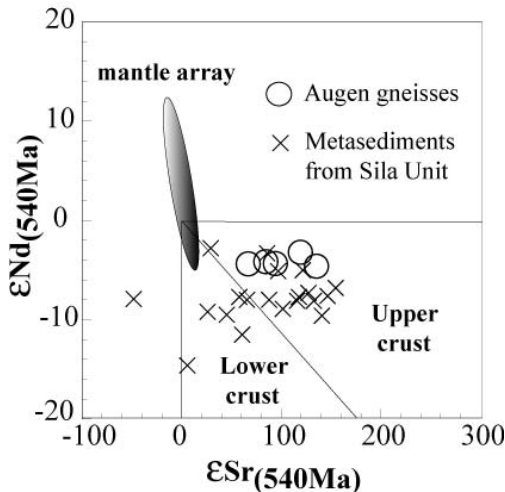


Fig. 7 –  $\epsilon Nd$  vs.  $\epsilon Sr$  plot. Augen gneisses (circles), metapelites of the lower crust of the Serre (crosses) and mantle array (De Paolo and Wasserburg, 1979) are reported. Data of metapelites from Del Moro *et al.*, (2000) and Caggianelli *et al.* (1991) recalculated at 540 Ma.

ORIGIN AND TECTONIC SETTING OF THE PROTOLITHS

The peraluminous character, the Rb-Sr isotopic signature and the similarity with the PAAS composition indicate a crustal involvement in the genesis of the augen gneisses. This is supported also by the occurrence of Archean, Palaeoproterozoic and Neoproterozoic inherited zircons (Micheletti *et al.*, 2007), and by the results of the dehydration melting experiments whose partial melts are characterized by distinct chemical signatures able to recognize the crustal sources (e.g. Patino Douce, 1999; Altherr and Siebel, 2002). The Calabria augen gneisses appear to be derived from partial melting of pelite-greywackes mixtures (Fig. 6). Strongly peraluminous granitic melts with significant contents of Fe, Ti, Mg and silica lower than 70 wt% differ significantly from crustal melts obtained experimentally during

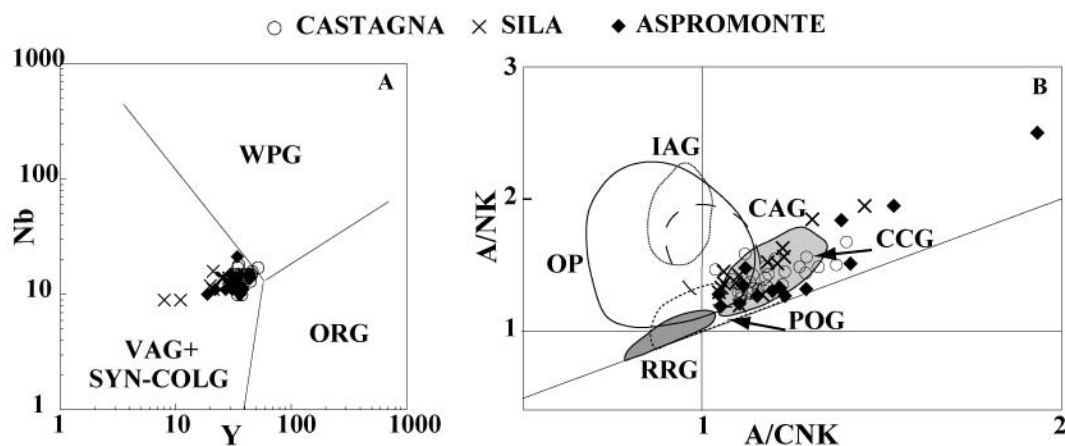


Fig. 8 – Plate-tectonic discrimination diagrams of granites. (A) Nb vs. Y plot (after Pearce *et al.*, 1984); VAG: volcanic arc granites; SYN-COLG: syn-collisional granites; WPG: within plate granites; ORG: ocean ridge granites. (B): A/NK vs. A/CNK diagram (after Maniar and Piccoli, 1989); OP: oceanic plagiogranites; IAG: island-arc granitoids; CAG: continental arc granitoids; RRG: rift-related granitoids; POG: post-orogenic granitoids; CCG: continental collision granitoids.

partial melting of metasediments (Patino Douce 1999). Thus the protoliths of augen gneisses represent, more likely, hybrid melts resulting from mixing of crust and mantle components or incomplete unmixing magma-restite (Patino Douce, 1999). The analysed augen gneisses show relatively high FeO\* (2 - 6 wt%), MgO (0.56 - 3.47 wt%), TiO<sub>2</sub> (0.33 - 1.16 wt%) and SiO<sub>2</sub> (64 - 75 wt%) (Table 1). In Fig. 6, the mixing patterns of crustal melts with increasing mantellic magma contributions under high and low pressures from Patino Douce (1999), as well as the trend of melt-restite mixing are given. The studied augen gneisses appear to be derived from crustal magmas, containing restitic components, mixed with mantle magma under low pressures. The pyrolite and PAAS normalized multi-element plots (Figs. 5B and 5C), due to the common negative and positive anomalies, confirm hybridization between crust and mantle melts. The spectrum of (<sup>87</sup>Sr/<sup>86</sup>Sr)<sub>i</sub> ratios and εNd values also point to a mantle contribution in the genesis of the igneous protoliths of the augen gneisses. This appears clearly from Fig. 7, where the augen gneisses plot along a possible mixing trend between mantle and crustal derivatives. The covariance TiO<sub>2</sub> (wt%) - Zr (ppm) (Fig. 4) suggests that restitic biotite played some

role in the present chemistries of the augen gneisses. In fact, biotite, which may include small zircons, is the unique Ti-bearing mineral in the studied rocks. Different degree of crust partial melting, different restite-melt separation and different proportions of two-component mixing might account for the chemical and isotopic characteristics of the studied augen gneisses. Melting-Assimilation-Storage-Homogenization (MASH in Hildreth and Moorbath, 1988) processes in the Precambrian basement possibly controlled the formation of the magma-batches, which coalesced to form the huge plutons. The Y-Nb plots (Pearce *et al.*, 1984), elsewhere able to discriminate among the tectonic settings of the granitic melt-emplacment, is here poorly informative, since the data points, as commonly happens for the granitoids, fall near the triple point (Fig. 8A). More indicative appears to be the A/CNK-A/NK diagram (Maniar and Piccoli, 1989) in which the augen gneisses point to an orogenic and collisional or post-collisional context (Fig. 8B). Following Patino Douce (1999), who suggests the low-pressure formation of the S-type peraluminous hybrids, it is possible to frame the emplacement of the protoliths of the augen gneisses from Calabria basement within a collapsed intracontinental orogen.

## DISCUSSION AND CONCLUSIONS

U-Pb data of magmatic zircons from the analysed augen gneisses give consistent *concordia* and *discordia* (lower intercept) ages (Micheletti *et al.*, 2007), suggesting the emplacement of the magmatic protolith in the time span between  $562 \pm 15$  Ma and  $526 \pm 10$  Ma. This limited range for the intrusion ages and the consistent geochemical signatures suggest a common genetic process for the different magma batches which coalesced to form the plutons. The peraluminous character, the similarities with the PAAS composition and the Rb-Sr and Sm-Nd isotope signatures indicate a crustal involvement in the formation process, which is further supported by the presence in the zircons of Archean, Palaeoproterozoic and Neoproterozoic inherited domains (Micheletti *et al.*, 2007). The protoliths are broadly compatible with involvement of magmas formed by dehydration melting of a metapelite-metagreywacke mixture in the source. However, the relatively high contents in FeO, MgO and TiO<sub>2</sub>, when compared to those from the experimental melts derived from metasedimentary sources, exclude the protoliths of the augen gneisses were pure crustal melts (see discussion in Patino Douce, 1999). The relatively low (<sup>87</sup>Sr/<sup>86</sup>Sr)<sub>i</sub> ratios and the εNd values, their significant variability among samples from a given unit, the coherence between PAAS and pyrolite multi-element normalized diagrams, such as the very large volumes of the augen gneisses favour a hybrid nature of the protoliths in the MASH system (Hildreth and Moorbath, 1988). Probably, the separation of the crustal melt from its restite was incomplete as appears from the distribution of the data points in Fig. 6, where the trends, calculated for different degree of crust-mantle magma mixing and different degree of melt-restite unmixing are reported (Patino Douce, 1999). The multi-element pyrolite-normalized plot, showing negative anomalies for Ba, Nb, Ta, Sr, P and Ti and positive ones for Th, U, K and Pb (Fig. 5b), suggests contribution from mantle-derived magmas in an orogenic setting. The high-K calc-alkaline to shoshonitic nature (Fig. 4) and the relationships apparent in the A/CNK vs. A/NK plot (Fig. 8b) also point to an

orogenic context, probably at the transition from compressional to extensional tectonics (e.g. Lameyre, 1988; Bonin *et al.*, 1998; Barbarin, 1999) or even after the tectonic collapse of an intracontinental orogen (Patino Douce, 1999) during the Neoproterozoic-Cambrian stage (570-520 Ma) of the amalgamation of Cadomian terranes to the Gondwana craton (Neubauer, 2002). The coeval intrusions of roughly similar batches of hybrid magmas indicate that the basements here considered were portions of the same Precambrian block.

Since the volume of the augen gneisses in the Castagna and Aspromonte Units is very significant, but very limited in the lower crust segment of the Sila Unit, the partial melting of metapelites, presently exposed in lower crust of the Serre, might have contributed to the magma genesis of the protoliths of the augen gneisses, which migrated upward, as suggested by Schenk (1990). However, the following points must be taken into consideration: i) most metapelites of the lower crustal section at present exposed have undoubtedly lower εNd values and almost 50% of the samples have also distinctly lower εSr values than the augen gneisses (Fig. 7); 2) zircon spot analyses from the metapelites do not show Archean and Palaeoproterozoic inheritance (Micheletti *et al.*, 2007) which are common for the augen gneisses; 3) the augen gneisses show homogeneous Nd model ages between 1.5-1.7 Ga, which may result from a mixing between Archean, Palaeoproterozoic and Neoproterozoic components in the source, whereas the metapelites presently exposed in the lower crust of the Serre show Nd model ages of 1.3 Ga from a megasample (Schenk 1989) or ranging from 1.8 to 2.5 Ga for seven specimens (Caggianelli *et al.*, 1991). Accordingly, it is difficult to derive the crustal component of the protoliths of the augen gneisses from the metapelites now exposed in the lower crust of the Serre. More likely, the formation of the crustal magmatic component involved a different crustal source, recording recycled terranes of the West African Craton (Gasquet *et al.*, 2005). After the initial stages of Cambrian rifting of the Gondwana margin, the pre-Variscan blocks, which have been later involved in the formation of the Variscan chain, underwent a complex

plate-tectonic evolution before the building of the Variscan chain (von Raumer *et al.*, 2003). So the Calabrian Units, containing pre-Variscan augen gneisses, probably originated from the original crustal roots involved in the formation of the felsic melts and became upper, middle and lower crust segments in the Variscan chain, respectively.

#### ACKNOWLEDGEMENTS:

D. Gasquet, an anonymous reviewer and the Editors are gratefully acknowledged for their criticism. This study was financially supported by the University of Bari (Grant 2005 Piccarreta).

#### REFERENCES

- ACQUAFREDDA P., LORENZONI S. and ZANETTIN LORENZONI E. (1994) – *Palaeozoic sequences and evolution of the Calabrian-Peloritani Arc (Southern Italy)*. Terra Nova, **6**, 582-594.
- ALTHERR R. and SIEBEL W. (2002) – *I-type plutonism in a continental back-arc setting: Miocene granitoids and monzonites from the central Aegean Sea, Greece*. Contrib. Mineral. Petrol., **143**, 397-415.
- BARBARIN B. (1999) – *A review of the relationships between granitoid types, their origins and their geodynamic environments*. Lithos, **46**, 605-626.
- BONARDI G., CAVAZZA W., PERRONE V. and ROSSI S. (2001) – *Calabria-Peloritani terrane and northern Ionian Sea*. In: Vai G.B. and Martini I.P. (Eds.), *Anatomy of an Orogen: the Apennines and Adjacent Mediterranean Basins*. Kluwer Acad. Publ., Great Britain, 287-306.
- BONARDI G., COMPAGNONI R., MESSINA A. and PERRONE V. (1984) – *Riequilibrizioni metamorfiche di probabile età Alpina nell'Unità dell'Aspromonte – Arco Calabro – Peloritano*. Rend. Soc. It. Mineral. Petrol., **39**, 613-628.
- BONIN B., AZZOUNI-SEKKAL A., BUSSY F. and FERRAG S. (1998) – *Alkali-calcic and alkaline post-orogenic (PO) granite magmatism: petrologic constraints and geodynamic settings*. Lithos, **45**, 45-70.
- BORSI S. and DUBOIS R. (1968) – *Données géochronologiques sur l'histoire hercynienne et alpine de la Calabre centrale*. C. R. Acad. Sci., Paris, **266**, 72-75.
- BOZKURT E., WINCHESTER J.A. and PARK R.G. (1995) – *Geochemistry and tectonic significance of augen gneisses from the southern Menderes Massif (West Turkey)*. Geol. Mag., **132**, 287-301.
- CAGGIANELLI A. and PROSSER G. (2002) – *Modelling the thermal perturbation of the continental crust after intraplate of thick granitoid sheets: a comparison with the crustal sections in Calabria (Italy)*. Geol. Mag., **139**, 699-706.
- CAGGIANELLI A., DEL MORO A., PAGLIONICO A., PICCARRETA G., PINARELLI L. and ROTTURA A. (1991) – *Lower crustal granite genesis connected with chemical fractionation in the continental crust of Calabria (Southern Italy)*. Eur. J. Mineral., **3**, 159-180.
- COLONNA V. and PICCARRETA G. (1976) – *Contributo alla conoscenza dell'Unità di Castagna in Sila Piccola: rapporti tra micascisti, paragneiss e gneiss occhiadini*. Boll. Soc. Geol. It., **95**, 39-48.
- DEL MORO A., FORNELLI A. and PICCARRETA G. (2000) – *Disequilibrium melting in granulite-facies metasedimentary rocks of the Northern Serre (Calabria-Southern Italy)*. Mineral. Petrol., **70**, 89-104.
- DE PAOLO D.J. and WASSERBURG G.J. (1976) – *Nd isotopic variations and petrogenetic models*. Geophys. Res. Lett., **3**, 249-252.
- DE PAOLO D.J. and WASSERBURG G.J. (1979) – *Petrogenetic mixing models and Nd-Sr isotopic patterns*. Geochim. Cosmochim. Acta, **43**, 615-627.
- FESTA V., MESSINA A., PAGLIONICO A., PICCARRETA G. and ROTTURA A. (2004) – *Pre-Triassic history recorded in the Calabria-Peloritani segment of the Alpine chain, southern Italy. An overview*. In: Castelli D. and Cesare B. (Eds.), *A showcase of the Italian research in metamorphic petrology*. Per. Mineral., **73/2** (Spec. Issue), 57-71.
- FORNELLI A., MICHELETTI F. and PICCARRETA G. (2007) – *Timing constraints for Variscan evolution of the lower crustal segment of the Serre (Calabria)*. Geitalia 2007, Epitome, p. 273.
- GASQUET D., LEVRESSE G., CHELLETZ A., AZIZI-SAMIR M.R. and MOUTTAQI A. (2005) – *Contribution to a geodynamic reconstruction of the Anti-Atlas (Morocco) during Pan-African times with the emphasis on inversion tectonics and metallogenic activity at the Precambrian-Cambrian transition*. Precamb. Res., **140**, 157-182.
- GRAESSNER T. and SCHENK V. (1999) – *Low pressure metamorphism of Palaeozoic pelites in the Aspromonte, southern Calabria: constraints on the thermal evolution in the Calabrian crustal cross-sections during the Hercynian orogeny*. J. Metam. Geol., **17**, 157-172.
- GRANDE A. and MICHELETTI F. (2006) – *Le metapeliti di medio-alto grado in Aspromonte meridionale:*

- aspetti dell'evoluzione tettono-metamorfica*. Abstract, Atti 85° Congr. Soc. It. Min. Petrol. Fluminimaggiore (CA).
- HILDRETH W. and MOORBATH S. (1988) - *Crustal contributions to arc magmatism in the Andes of Central Chile*. Contrib. Mineral. Petrol., **98**, 4, 455-489.
- LAMEYRE, J. (1988) - *Granite settings and tectonics*. Rend. Soc. It. Mineral. Petrol., **43**, 215-236.
- LE MAITRE R.W., BATEMAN P., DUDEK A., KELLER J., LAMEYRE J., LE BAS M.J., SABINE P.A., SCHMID R., SORENSEN H., STRECKEISEN A., WOOLEY A.R. and ZANETTIN B. (1989) - *Classification of igneous rocks and glossary of terms*. Blackwell scientific publications, Oxford. 193 pp.
- MACLEAN W.H. and BARRET T.J. (1993) - *Lithogeochemical techniques using immobile elements*. J. Geochem. Expl., **48**, 109-133.
- MANIAR P.D. and PICCOLI P.M. (1989) - *Tectonic discrimination of granitoids*. Geol. Soc. Am. Bull., **101**, 635-643.
- MC DONOUGH W.F. and SUN S. (1995) - *The composition of the Earth*. Chem. Geol., **120**, 223-253.
- MESSINA A., RUSSO S., BORCHI A., COLONNA V., COMPAGNONI R., CAGGIANELLI A., FORNELLI A. and PICCARRETA G. (1994) - *Il Massiccio della Sila, settore settentrionale dell'Arco Calabro-Peloritano*. Boll. Soc. Geol. It., **113**, 539-586.
- MICHELETTI F., BARBEY P., FORNELLI A., PICCARRETA G. and DELOUË E. (2007) - *Latest Precambrian to Early Cambrian U-Pb zircon ages of augen gneisses from Calabria (Italy), with inference to the Alboran microplate in the evolution of the peri-Gondwana terranes*. Int. J. Earth Sci., **96**, 5, 843-860.
- NEUBAUER F. (2002) - *Evolution of late Neoproterozoic to early Paleozoic tectonic elements in Central and Southeast European Alpine mountain belt: review and synthesis*. Tectonophysics, **352**, 87-103.
- PAGLIONICO A. and PICCARRETA G. (1976) - *Le Unità del Fiume Pomo e di Castagna nelle Serre settentrionali (Calabria)*. Boll. Soc. Geol. It., **95**, 27-37.
- PATINO DOUCE A. E. (1999) - *What do experiments tell us about the relative contributions of crust and mantle to the origin of granitic magmas?* In: Castro A., Fernandez C. and Vigneresse J. L. (Eds.), *Understanding granites: Integrating new and classical techniques*. Geol. Soc., London, Special Publ., **168**, 55-75.
- PEARCE J.A., HARRIS N.B.W. and TINDLE A.G. (1984) - *Trace element discrimination diagrams for the tectonic interpretation of granitic rocks*. J. Petrol., **25**, 956-983.
- SCHENK V. (1980) - *U-Pb and Rb-Sr Radiometric Dates and their Correlation with Metamorphic Events in the Granulite-Facies Basement of the Serre, Southern Calabria (Italy)*. Contrib. Mineral. Petrol., **73**, 23-38.
- SCHENK V. (1984) - *Petrology of felsic granulites, metapelites, metabasics, ultramafics, and metacarbonates from Southern Calabria (Italy): Prograde metamorphism, uplift and cooling of a former Lower Crust*. J. Petrol., **25**, 255-298.
- SCHENK V. (1989) - *P-T-t path of the lower crust in the Hercynian fold belt of southern Calabria*. In: Daly J.S., Cliff R.A. and Yardley B.W.D. (Eds.), *Evolution of metamorphic belts*. Geol. Soc. Special Publ., **43**, 337-342.
- SCHENK V. (1990) - *The exposed crustal cross section of southern Calabria, Italy: structure and evolution of a segment of Hercynian crust*. In: Salisbury M.H. and Foutain D.M. (Eds.), *Exposed Cross-sections of the Continental Crust*. Kluwer Acad. Publ., The Netherlands, 21-42.
- SCHENK V. and TODT W. (1989) - *Age of formation of the southern calabrian crust*. Terra Abstracts, **1**, 350.
- SENESE G. (1999) - *Petrologia della zona di bordo delle plutoniti delle Serre (Catanzaro, Calabria)*. Unpubl. Ph.D. Thesis, Bari University (Italy), 80 pp.
- TAYLOR S.R. and MCLENNAN S.M. (1985) - *The continental crust: its composition and evolution. An examination of the geochemical record preserved in sedimentary rocks*. Blackwell scientific publications, Oxford, 312 pp.
- VON RAUMER J.F., STAMPELI G.M. and BUSSY F. (2003) - *Gondwana-derived microcontinents — the constituents of the Variscan and Alpine collisional orogens*. Tectonophysics, **365**, 7-22.